



Synthetic Aperture Radar Image Super Resolution Using Deep Learning Based on Modified CNN With Rectified Linear Unit6 (RELU6)

¹Shubham Dwivedi, ²Dr. Babita Pathik,

¹M.Tech Student (IT), ²Professor

¹ Department of Information Technology, ²Department of Computer Science Engineering

^{1,2} Technocrats Institute of Technology, RGPV, Bhopal (M.P.), INDIA

Abstract : In The super resolution (SR), the method of obtaining an image with high resolution (HR) through processing a low-resolution (LR) picture, being the primary concern of the present research. During single image super resolution (SISR), the improved very deep super resolution (IVDSR) was used to deliver an improved version of the SISR. The suggested approach depends on CNN, for instance, with a network depth of 20 and several image attributes to train that include apply up-sampling as well as residual images—a vital phase in SISR. The bi-cubic approach and the suggested deep learning based on Modified CNN with rectified linear Unit 6—are combined to enhance the methodology that is being described. The methodology that will be considering determines improved PSNR and SSIM outcomes. Both of these factors are crucial for the final results analysis of the image super resolution (ISR) research. Testing data sets, such as the UC Meced land collection, are available for the training and testing of the approach given. When compared to other prior techniques, the suggested technique produces superior results. According on the WHU-RS19 dataset set, the suggested method's output will be compared to that of SRCNN, VDSR, D-DBPN, RCAN, SRFBN, SAN, Hybrid Method [1], and the proposed MSISR. Use MATLAB 2020A for the suggested method's simulation.

IndexTerms - Super Resolution, Deep Neural Network, Image Super Resolution, Convolution Neural Network, Remote Sensing Image, Up Sampling, Residual.

I. INTRODUCTION

SISR has been a key topic among scientists in the last few years. Single-image super-resolution and other methods have been created to identify various high-resolution images. These solutions seem to be very reliant on a variety of circumstances as well as unique datasets and observations. Single-image super resolution is shown in the following fig.1."Super-resolution" is the process of converting low-resolution images into high-resolution images (SR). Therefore, to put it differently, LR stands for a single image input, high-resolution for the real data, and SR for the predicted high-resolution.



Fig. 1. Shows the Single Image Super Resolution (SISR) [12]

Image super resolution is well know problem for satellite image as well as synthetic aperture radar images (SAR). The main objective of proposed research work to improve the visual quality of satellite and SAR images. [27]. The research and technique of receiving information about an item, region, or phenomena by processing results collected by a machine that is not in communication with the subject, place, or activity being researched is known as "remote sensing" [20]. The remote sensing picture, collected by sensor spectral remote sensing techniques, provides a lot of information for monitoring the land temperature, and has a wide spectrum of uses in the areas of image corresponding and sensing, land surface identification, urban economic evaluation, energy investigation, and so on [19]. High-resolution satellite images have been shown to serve a vital function. But compared to synthetic photographs, remote sensing photography has less resolution and geographic clarity because of things like long-distance imaging, unstable weather, broadcast distortion, and mobility distortion.. The scales of surface elements in remotely sensed photography are also often different, which makes the items and their surroundings work together in the combined distribution of their picture patterns [18].

A. Single Image Super Resolution

An A super-resolution network, as seen in fig. 1, at the earth's cubic, may be employed in a variety of procedures. It will be used to improve the process of categorizing photographs and make it simpler for users. They spend several hours subdividing automobiles or categorizing military aircraft, so improving the quality of the photos they're viewing speeds up their job, improves the quality of their categorization, and improves their overall well-being [14]. It is something that a large number of individuals might benefit from as well. This improvement may be beneficial to people as well as robots. The purpose of single image super-resolution (SISR) is to boost image resolution beyond the limitations of the sensor. That also means growing in terms of visual elements without maintaining greater location data than the initial acquisition equipment acquired. There are two types of SR approaches, single-image and multi-image, that may be used according to the input pictures. Multi-image SR methods need numerous scene images to be obtained concurrently at various places, while single-image SR approaches employ a single image of the target scene to get the super-resolved output [15]. The single-image technique is often used in remote sensing because it gives a more flexible strategy for super-resolving any kind of imaging sensor without requiring a satellite constellation. This problem is usually solved by using strong information from a group of images to narrow down the number of possible solutions.

II. LITERATURE SURVEY

Yu, Fanghua, Xintao et.al. (2023). "OSRT: Omnidirectional image super-resolution with distortion-aware transformer." In this research work, authors find that the previous downsampling process in the ODISR task harms the intrinsic distribution of pixel density in ODIs, which leads to poor generalization ability in real-world scenarios. To tackle this issue, we propose Fisheye down sampling, which mimics the real-world imaging process to preserve the realistic density distribution. After refining the down sampling process, we design a distortion-aware Transformer (OSRT) to modulate distortions continuously and self-adaptively. OSRT learns offsets from the distortion-related condition and rectifies distortion by feature-level warping. Moreover, to alleviate the overfitting problem of large networks, we propose to synthesize additional ERP training data from the plain images. Extensive experiments have demonstrated the state-of-the-art performance of our OSRT [1].

Zhang, et.al. (2022), "Single-Image Super Resolution of Remote Sensing Images with Real-World Degradation Modeling", In this article, a real-world degradation modeling framework and a residual balanced attention network with modified UNet discriminator (RBAN-UNet) have been presented for remote sensing image super resolution. The quality of real RSIs is affected by a series of factors, such as illumination, atmosphere, imaging sensor responses, and signal processing, resulting in a gap in the performance of previous methods between laboratory conditions and actual conditions. To model the real-world degradation of RSIs, researcher presented to estimate the blur kernels and noise patches in the dataset separately. Then, the blur kernels and noise patches Researcher used to construct a realistic dataset that follows the desired mapping function from realistic LR images to clean HR images. Moreover, researcher develop a novel CNN model to perform the SR reconstruction for RSIs. Researcher use a residual in residual architecture as the backbone and embed balanced attention modules (BAM) to improve the performance. To generate more realistic results, a modified UNet pixel-wise discriminator is employed. Detailed experiments were carried out to compare the presented model with classic SISR networks. Referenced experiments, non-referenced experiments, and ablation studies validate that the degradation modeling framework improves the performance of models dealing with real RSIs and the presented RBAN UNet model achieves a state-of-the-art performance in the real-world SISR problem for RSIs [2].

Zili, et.al. (2022), "Unsupervised Remote Sensing Image Super-Resolution Guided by Visible Images", In this research work presented a novel cross-domain super-resolution method called UVRSR, which allowed training to be conducted with unpaired HR visible images and LR remote sensing images. It enhanced the capability for HR visible images to assist in the reconstruction of remote sensing images. It is the first work to apply visible images to assist remote sensing domain SR, and is also the first to perform cross-domain SR without HR/LR training pairs. It combines the advantages of HR visible images and remote sensing images, or, in other words, the advantages of visible realistic details and remote sensing structural information. In UVRSR, to learn more detailed images without domain shift in the reconstruction, researcher presented a novel two-branch training strategy and a domain ruled discriminator. The two-branch training, which included the visible image-guided branch (VIG) and the remote image-guided branch (RIG), has different functions for the SR network. VIG is designed to explore sufficient high frequency information from the HR visible target, while RIG is meant to learn the inner relationship in the remote sensing domain [3].

Wang, et.al, (2022) "Remote sensing image super-resolution and object detection: Benchmark and state of the art." The object localization and detection task in RS images is a topic of continuous research; thus, developing state-of-the-art object detectors for remote sensing of the environment is of utmost. In this research work presented a new benchmark RSSOD dataset for remote sensing object detectors with a high overlap of classes and complex settings, emphasizing small-sized objects. Researcher also presented an RFA-based MCGR network that achieved state-of-the-art image SR quality and object detection tasks. The current detection accuracy for the classes like vehicle, airplane, and ship Researcher satisfactory, while there needs further exploration to learn the complex features of the tree and low-vegetation classes. Extensive experiments show that using an image SR network before the object detection task helps in improving the map for object detection, and the presented MCGR outperforms the state-of-the-art YOLOv5 for map by 5% and 13% for scale factors of 2 and 4, respectively [4].

Jia, S., et.al, (2022). In this research, researcher present a GAN-based SR network named the multi-attention-GAN that correctly learns the mapping from LR to HR images to generate perceptually pleasing HR images. Specifically, researcher first designed a GAN-based framework for the image SR task. The key to accomplishing the SR task is the image generator with post-up-sampling that researcher designed. The main body of the generator contains two blocks; one is the PCRDB block, and the other is the AUP block. The AttPConv in the PCRDB block is a module that combines multi-scale convolution and channel

attention to automatically learn and adjust the scaling of the residuals for better results. The AUP block is a module that combines pixel attention to perform arbitrary multiples of up-sampling. These two blocks work together to help generate better quality images. For the loss function, researcher design a loss function based on pixel loss and introduce both adversarial loss and feature loss to guide the generator learning. Finally, it is demonstrated by researcher experiments that researcher presented MA-GAN can perform better than some state-of-the-art SR methods [5]. *Zhang, et.al, (2020)*, "Remote sensing image super-resolution via mixed high- order attention network", In this article, researcher presented a novel network for remote sensing image SR named MHAN to fully exploit hierarchical features by applying different order HOA modules to feature maps with different frequency bands. Compared with commonly use CA, the presented HOA module is capable of modeling complex and high-order statistics. Due to the weighted channel wise concatenation (WCC), CG and CB can adaptively adjust the ratio between the nonlinear and identity mapping branches, hence extending the model representational capacity. Moreover, FAC is also presented to connect the feature extraction and feature refinement networks effectively. The comprehensive experimental results have demonstrated that researcher MHAN could provide the better performance in comparison with the state-of-the-art methods by using less running time and GPU cost [6]. *Li, et.al. (2019)*, "**Feedback network for image super-resolution**", In this research, researcher a novel network for image SR called super-resolution feedback network (SRFBN) to faithfully reconstruct a SR image by enhancing low-level representations with high-level ones. The feedback block (FB) in the network can effectively handle the feedback information flow as well as the feature reuse. In addition, a curriculum learning strategy is presented to enable the network to well suitable for more complicated tasks, where the low-resolution images are corrupted by complex degradation models. The comprehensive experimental results have demonstrated that the presented SRFBN could deliver the comparative or better performance in comparison with the state-of-the-art methods by using very fewer parameters [7].

III. DEEP LEARNING AND MACHINE LEARNING

Deep In this section discuss the proposed solution for **Synthetic Aperture Radar Image Super Resolution Using Deep Learning Based on Modified CNN With Rectified Linear Unit6 (RELU6)** . The proposed solution which solve the problem of previous work that is discuss in the previous research works. The proposed method is design to enhance the resolution of image using single image super-resolution (SISR). The suggested technique is extensively used in computer vision applications, which span from processing high resolution images needed for in-depth disease investigation to security and surveillance imaging. The three main issues with single picture super-resolution are similarity mismatch, blur, and fine edge recognition. The two backbone outcome parameters in the suggested study are the measurement of the structural similarity index and the peak signal to noise ratio.

For the calculation of accuracy of proposed method required both data training and testing data sets. In the first part of proposed method create training data set and in the second stage apply Convolutional Networks (CNN) with Relu6 calculation.

Synthetic Aperture Radar Image Super Resolution Using Deep Learning Based on Modified CNN With Rectified Linear Unit6 (RELU6) Training Stage - Training is the important part of proposed single image super-resolution (SISR) method. In the below section discuss the training.

Training Steps

1. Data Set Selection - In this step selection of the 'data set'. There are different data set available for training. As per requirement of work select the data set. In the data set there are different images available in the different format such as 'jpg', 'bmp' and 'png'.
2. Preprocessing of Selected data - In this step apply preprocessing of the selected image from selected data set. Apply list creation of training images.
3. Create list of all images available in data set. Apply Up sampling of images presented in the current directory as well as apply calculate residual of the network.
4. Define different resolution factor [2,3and 4], Now start the proposed MSISR training for this require three parameters scale factor, up sampled directory and residual outcome image directory name.
5. Apply Patch in training images and store in random patch data store.
6. Now apply deep neural network with depth of 20 and apply convolution 2d with layer(3,64) and also apply 'Weights Initializer', 'Histogram equalization', 'Bias Initializer', of the convolution 2d network.
7. Now apply the middle layers that is convolution of the intial layer and residual Layer.
8. In the the convolution 2D networ final layer that is genrate by ther Conv Layer and regression Layer
9. Now apply the layers combination that is first Layer, middle Layers,and final Layers with the number of epochs is100 and learning rate factor is 0.1 and minimize batch size is 64. Finally calculate the image (Iycbcr).
10. Apply the combination of the Fusion = Iy bicubic + Iresidual; // Bicubic image and Residual Image Obtain the CNNREL6= ycbcr2rgb(cat(3,Isr, Icb bi cubic, Icr bi cubic)); Show Image (Ivdsr)

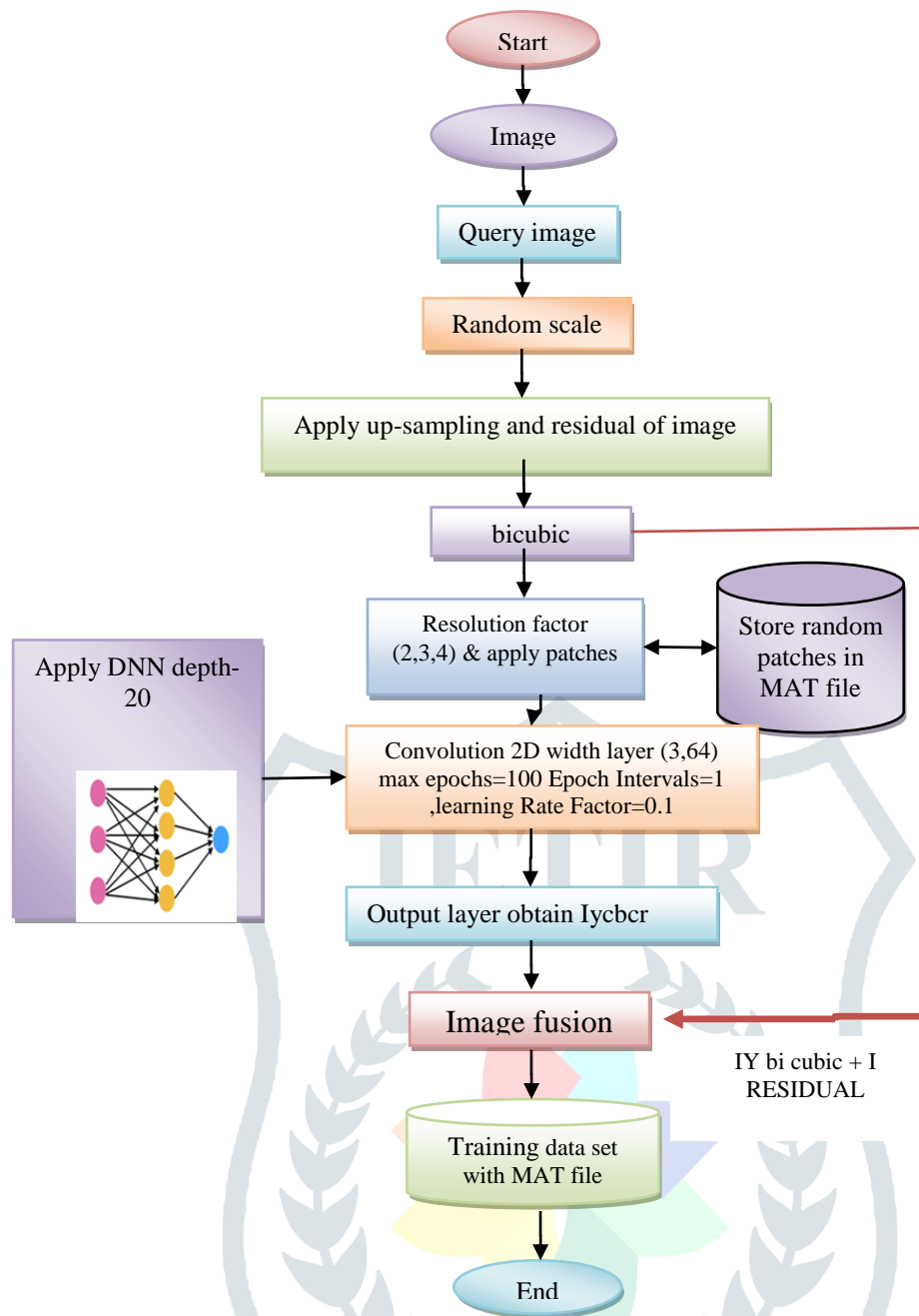


Fig.2: Training data set Flow diagram

Rectified linear unit

Rectified linear unit, also known as ReLU, is an acronym that refers to a device that uses the non-saturating activation function. The capability of CNNs to generate the internal structure of a two-dimensional image is one of the advantages of utilizing these algorithms. When dealing with satellite images, it is essential that the model be capable of learning location but also scale in a variety of different data formats. This is made possible by the previous point.

Modified Relu6 Leaky ReLUs make it possible for a small positive gradient to exist even while the unit is inactive.

$$f(x) = \begin{cases} x, & \text{if } x > 0 \\ 0.01x, & \text{otherwise} \end{cases} \tag{1}$$

ReLU6

ReLU6 (ReLU6) take this idea one step advance by turning the coefficient of leakage into a variable that is knowing along with the other features of the neural net.

$$f(x) = \begin{cases} x, & \text{if } x > 0 \\ ax, & \text{otherwise} \end{cases} \tag{2}$$

and thus has a relation to "maxout" networks

$$f(x) = \max(x, ax) \tag{3}$$

Note that for $a \leq 1$, this is equivalent.

Examine scalar-valued, discrete temporal structures known as initially linear time invariant, or LTI, processes. This will enable us to comprehend the convolution operation's relevance. Any system that converts one sequence into another—which is what an LTI system does—has the two properties listed below. An LTI system is denoted by the symbol $O()$.

$x1(t)$ and $x2(t)$ and scalars $\alpha1$ and $\alpha2$,

$$O(\alpha_1 X_1(\cdot) + \alpha_2 X_2(\cdot))(t) \quad (4)$$

$$= \alpha_1 O(X_1(\cdot))(t) + \alpha_2 O(X_2(\cdot))(t) \quad (5)$$

Time invariance- input signal

$$X(\cdot)X(\cdot) \quad (6)$$

$$\text{Output } Y(\cdot) = O(X(\cdot))Y(\cdot) = O(X(\cdot)) \quad (7)$$

The time shifted input

$$\sim X(t) = X(t - \tau) \quad (8)$$

output

$$O(\sim X(t))O(X(t)) \quad (9)$$

Denoted

$$\sim Y(\cdot)Y(\cdot) \quad (10)$$

is the time-shifted output of the original input.

$$\sim Y(t) = Y(t - \tau) \quad (11)$$

LTI describes several signal operations effectively. Signal $X(t)$. It can be represented as,

$$X(t) = \int_{-\infty}^{\infty} X(\tau)\delta(t - \tau) \quad (12)$$

Where $\delta(t)$ is the sequence such that $\delta(0)=1$ and for $t \neq 0$, $\delta(t)=0$.

This version, together with the LTI properties:

$$Y(t) = O(X(t)) \quad (13)$$

$$= O(\int_{-\infty}^{\infty} X(\tau)\delta(t - \tau)) \quad (14)$$

$$= \int_{-\infty}^{\infty} X(\tau)O(\delta(t - \tau)) \quad (15)$$

The present denotes the output of $\delta(t)$ as $H(t)$. This is called the impulse response.

Time invariance

$$O(\delta(t - \tau)) = H(t - \tau) \quad (16)$$

Therefore arrive at

$$Y(t) = \int_{-\infty}^{\infty} X(\tau)H(t - \tau) \quad (17)$$

This operation, which is represented by the notation, is known as the convolution of $X(\cdot)$ and $H(\cdot)$. When considering linear time invariant systems, convolutions naturally arise because the action of the system on any given signal can be simply expressed as the convolution of the signal with the impulse response of the system. One may use commutativity to the convolution process. X times H hence equals H times X . Modifying the pertinent variables will make this task simple.

$$\tau' = t - \tau \quad (18)$$

$$X * H = \int_{-\infty}^{\infty} X(\tau)H(t - \tau) \quad (19)$$

$$= \int_{-\infty}^{\infty} X(t - \tau')H(\tau') = H * X \quad (20)$$

we were to define the convolution operation differently

$$X * H = \int_{-\infty}^{\infty} X(\tau)H(\tau - t) \quad (21)$$

IV. SIMULATION AND RESULT

We apply our proposed technique to the UC-Merced land data collection (UC-Merced) [15] as an illustration of its effectiveness. This data collection has been heavily used for research and development by the remote sensing SR community. In particular, the 21 classes that UC-Merced offers span a wide range of remote sensing applications, from baseball fields to the beach, from agriculture to aerial photography. There are 100 images in each category, with an average pixel size of 256 by 256 and a spatial resolution of around 0.3 meters [15]. The suggested approach is tested using the WHU-RS19 data set. Seven photos make up the dataset: fields, parking, industry, rivers, lakes, forests, and grass. A micro-form of the UC-Merced data collection is this one.

'UC-Merced land data set' The University of California, Merced is an outdoor use remote sensing picture collection consisting of 21 classes, each containing 100+ photos. Large photos from the USGS National Map metropolitan Area Imagery collection for different metropolitan locations around the US were manually used to extract the pictures. This public domain picture has a pixel resolution of 0.3 m. Although the majority of the photos are 256 by 256 pixels, 44 of them have distinct shapes. Homepage: <http://weegee.vision.ucmerced.edu/datasets/landuse.html>

'WHU-RS19' data set WHU-RS19 is a collection of high-resolution satellite photos up to 0.5 m that are exported from Google Earth. The following image shows a few examples from the database. High-resolution satellite images of 19 classifications of significant sceneries are included in it, including commercial, desert, agriculture, football fields, forests, industrial, meadows, mountains, parks, parking lots, ponds, ports, residential areas, rivers, viaducts, and beaches. There are around 50 examples per class. It's important to keep in mind that picture samples within the same class may differ in terms of size, orientation, and lighting since they are gathered from various places in satellite photos with varying resolutions.

PSNR Peak Signal to Noise Ratio (PSNR): The PSNR is computed as:

$$\text{PSNR} = 10 \log_{10} \frac{s^2}{\text{MSE}} \quad (22)$$

The PSNR is higher for an excellent worth image and lower for a poor quality image. It measures image fidelity, that is, however closely the distorted image resembles the actual image. In our research work on the basis of our image size 255x255.

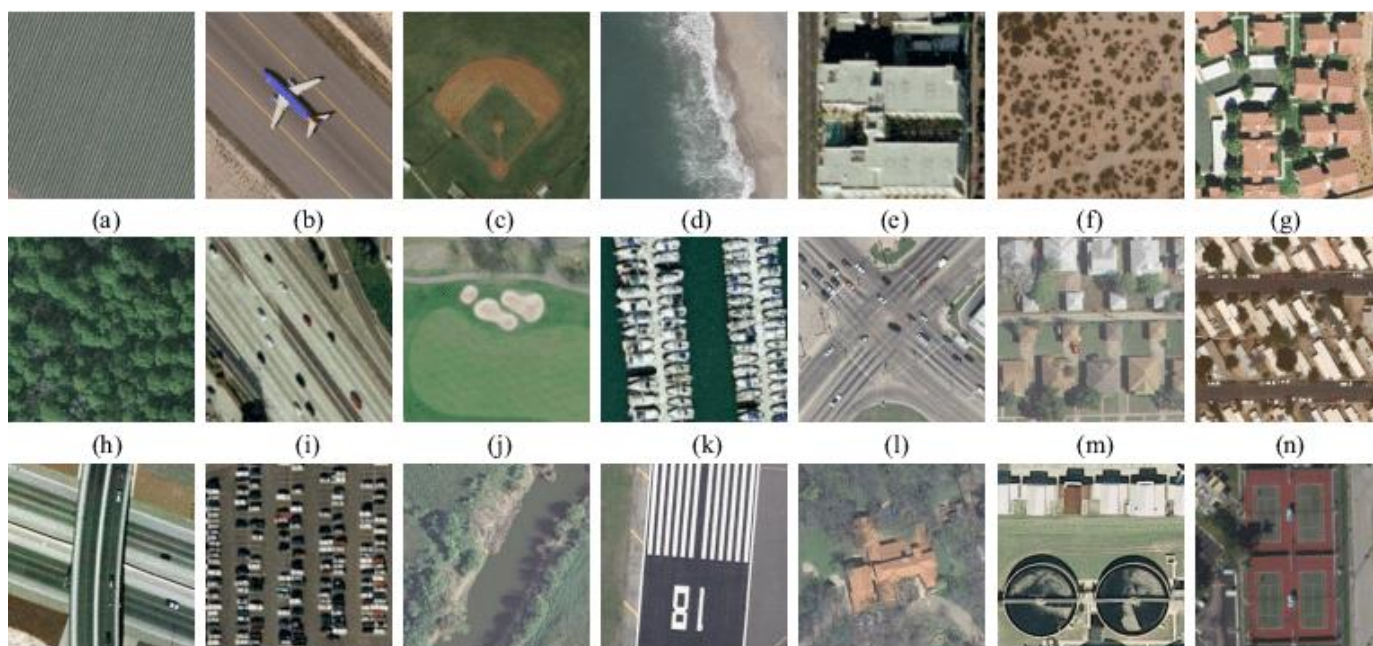
Mean Square Error (MSE): The MSE measures the standard amendment between the actual image (X) and the noised image (Y) and is given by:

$$\text{MSE} = \frac{1}{N} \sum_{j=0}^{N-1} (X_j - Y_j)^2 \quad (23)$$

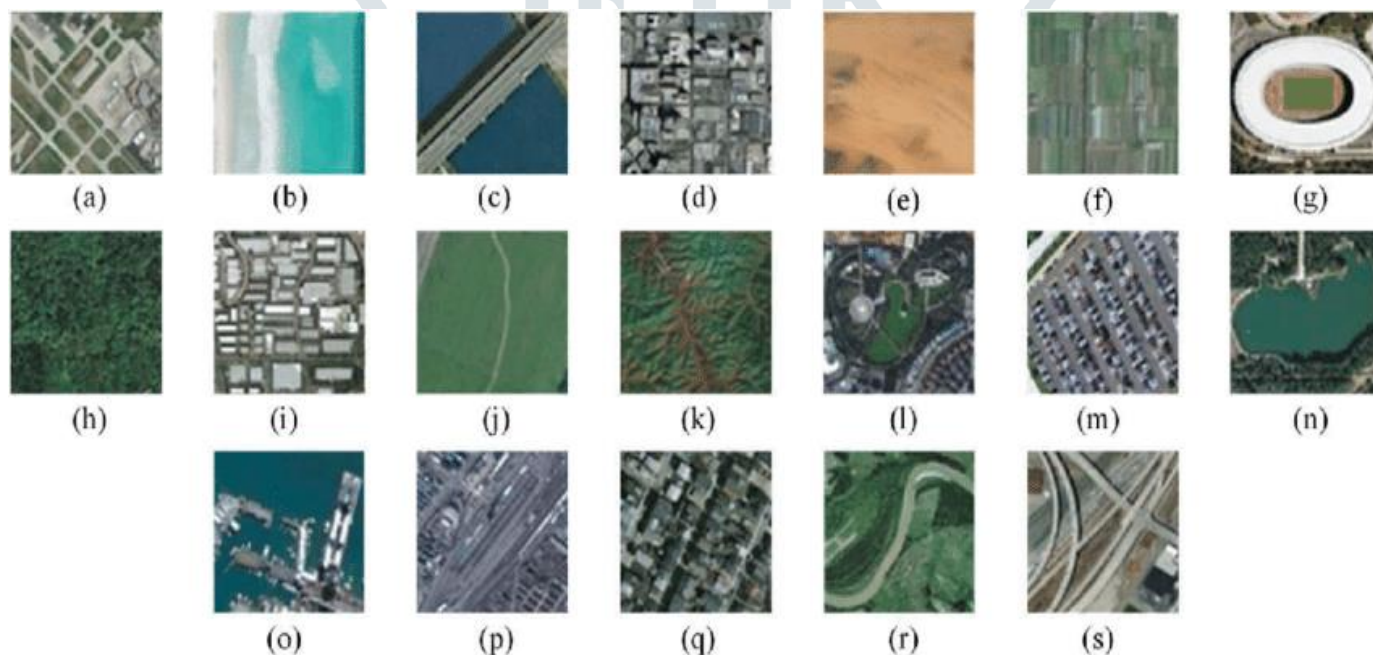
X_j Shows the cover image

Y_j Shows the stego image

The MSE has been extensively used to quantify image quality and once used alone; it doesn't correlate powerfully enough with sensory activity quality. It ought to be used, therefore in conjunction with alternative quality metrics and perception.



(a) Database of 'UC-Merced land data set (UC-Merced)'



(b) Data set of "WHU-RS19"

PSNR Peak Signal to Noise Ratio (PSNR): The PSNR is computed as:

$$PSNR = 10 \log_{10} \frac{s^2}{MSE} \tag{221}$$

The PSNR is higher for an excellent worth image and lower for a poor quality image. It measures image fidelity, that is, however closely the distorted image resembles the actual image. In our research work on the basis of our image size 255x255.

Mean Square Error (MSE): The MSE measures the standard amendment between the actual image (X) and the noised image (Y) and is given by:

$$MSE = \frac{1}{N} \sum_{j=0}^{N-1} (X_j - Y_j)^2 \tag{23}$$

X_j Shows the cover image

Y_j Shows the stego image

The MSE has been extensively used to quantify image quality and once used alone; it doesn't correlate powerfully enough with sensory activity quality. It ought to be used, therefore in conjunction with alternative quality metrics and perception.

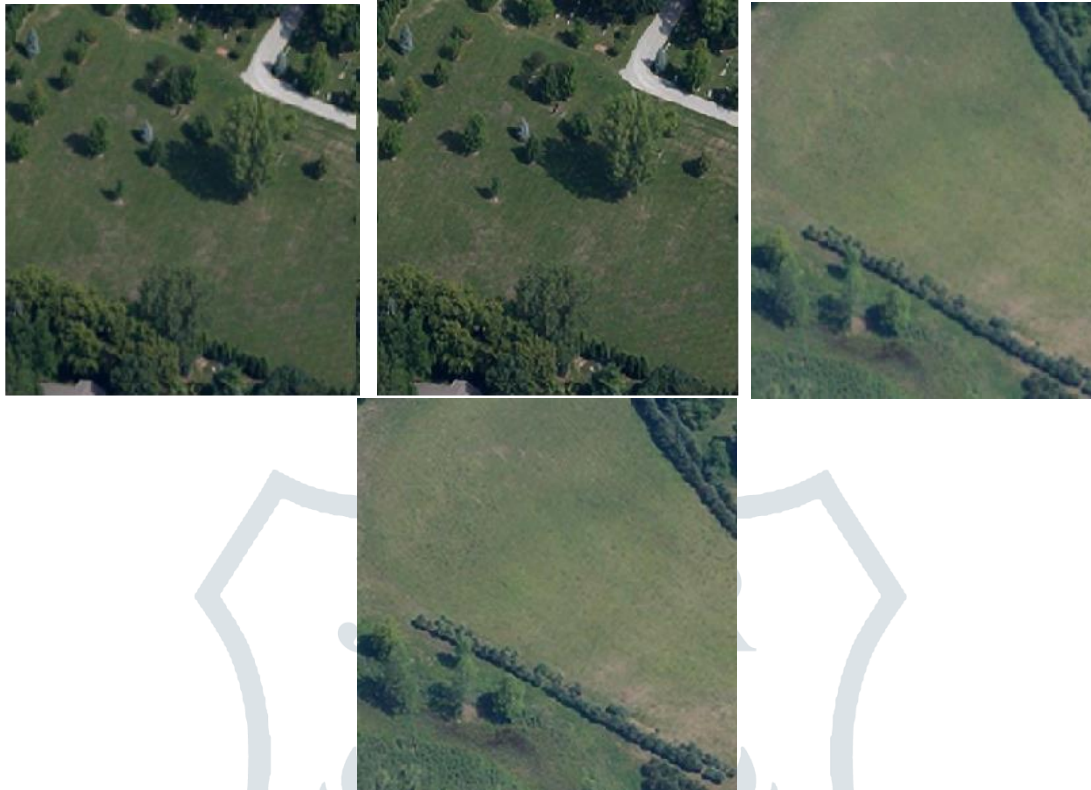
SSIM

$$SSIM(x, y) = [l(x, y)]^\alpha [c(x, y)]^\beta [s(x, y)]^\gamma \tag{24}$$

with respect to which are the mean values for the pictures of x , and cross-covariance is the standard deviation of the images. If $\alpha = 1$ (the default value for Exponents) and $C3 = C2/2$ (the default value for $C3$) are used, the index becomes:

$$SSIM(x, y) = \frac{(2\mu_x\mu_y + C_1)(2\sigma_{xy} + C_2)}{(\mu_x^2 + \mu_y^2 + C_1)(\sigma_x^2 + \sigma_y^2 + C_2)} \quad (25)$$

Result Discussion In this section discuss the MATLAB simulated outcomes in terms of qualitative research and quantities research. Now we will talk about the simulation result using the provided technique. In order to facilitate a visual comparison of the results, illustrated in fig. 5.5, Fig.5.5 depicts the many outputs that may be achieved using the suggested strategy on scale factor 2.



(a) GrassImage (a1) Enhanced grass image Field image (b1) Enhanced Field Image

In the above figure 5.5 shows the visual result comparison of proposed method with previous method. Now discuss the quantities analysis on two different result parameters PSNR and SSIM.

Table. I. Comparison of Proposed Method Different Previous Methods based on PSNR

WHU-RS19	SRCNN [14]	VDSR [12]	D-DBPN [11]	RCAN [13]	SRFBN [9]	SAN [5]	MHAN [10]	Proposed
Grass	38.66	38.96	39.20	39.27	39.17	39.21	39.27	37.43
Field	36.32	36.56	36.82	36.90	36.79	36.85	36.89	38.72
Industry	30.29	31.14	31.54	31.7	31.52	31.64	31.63	31.23
River Lake	34.99	35.40	35.59	35.65	35.58	35.63	35.64	36.20
Forest	32.61	32.75	32.85	32.88	32.84	32.87	32.88	35.11
Resident	29.55	30.23	30.53	30.64	30.52	30.61	30.61	32.06
Parking	29.01	29.54	30.08	30.24	30.07	30.18	30.18	31.21

Table. II. Comparison of proposed method different previous methods based SSIM

WHU-RS19	SRCNN [14]	VDSR [12]	D-DBPN [11]	RCAN [13]	SRFBN [9]	SAN [5]	MHAN [10]	Proposed
Grass	0.94	0.942	0.941	0.945	0.94	0.94	0.94	0.98
Field	0.862	0.865	0.871	0.871	0.86	0.87	0.87	0.98
Industry	0.895	0.909	0.915	0.917	0.91	0.91	0.91	0.93
River Lake	0.930	0.934	0.936	0.937	0.93	0.93	0.93	0.94

Forest	0.870	0.873	0.876	0.87	0.87	0.87	0.87	0.89
Resident	0.867	0.903	0.908	0.91	0.90	0.90	0.91	0.93
Parking	0.867	0.879	0.892	0.89	0.89	0.89	0.89	0.94

V. CONCLUSION

The present research offers SAR picture quality enchantment and super-resolution for satellite photos. The present method uses CNN to fuse the features of two separate techniques for training purposes, with a network depth of 20 and up-sampling and residual pictures employed during training (a critical step in SISR). It is shown that combining VSDR methods with the characteristics of the bi-cubic approach is necessary to improve the present outcome. For the improvement of the proposed Synthetic Aperture Radar Image Super Resolution Using Deep Learning Based on Modified CNN With Rectified Linear Unit6 (RELU6) . The presented method shows better results in terms of PSNR and SSIM. There are data sets available for the training and testing of the presented method, such as test datasets UC Meced land Data set. The result of proposed method is based on WHU-RS19 data set and result compared with SRCNN, VDSR, D-DBPN, RCAN, SRFBN, SAN, Hybrid Method [1] and Proposed MSISR. For the simulation of proposed method use MATLAB 2020A.

REFERENCES

- [1] Yu, Fanghua, Xintao Wang, Mingdeng Cao, Gen Li, Ying Shan, and Chao Dong. "OSRT: Omnidirectional image super-resolution with distortion-aware transformer." In *Proceedings of the IEEE/CVF Conference on Computer Vision and Pattern Recognition*, pp. 13283-13292. 2023.
- [2] Carlson, Zhang, Jizhou, Tingfa Xu, Jianan Li, Shenwang Jiang, and Yuhan Zhang. "Single-Image Super Resolution of Remote Sensing Images with Real-World Degradation Modeling." *Remote Sensing* 14, no. 12 (2022): 2895.
- [3] Zhang, Zili, Yan Tian, Jianxiang Li, and Yiping Xu. "Unsupervised Remote Sensing Image Super-Resolution Guided by Visible Images." *Remote Sensing* 14, no. 6 (2022): 1513.
- [4] Wang, Yi, Syed Muhammad Arsalan Bashir, Mahrukh Khan, Qudrat Ullah, Rui Wang, Yilin Song, Zhe Guo, and Yilong Niu. "Remote sensing image super-resolution and object detection: Benchmark and state of the art." *Expert Systems with Applications* (2022): 116793.
- [5] Jia, Sen, Zhihao Wang, Qingquan Li, Xiuping Jia, and Meng Xu. "Multi- Attention Generative Adversarial Network for Remote Sensing Image Super Resolution." *IEEE Transactions on Geoscience and Remote Sensing* (2022).
- [6] Zhang, Dongyang, Jie Shao, Xinyao Li, and Heng Tao Shen. "Remote sensing image super-resolution via mixed high-order attention network." *IEEE Transactions on Geoscience and Remote Sensing* 59, no. 6 (2020): 5183-5196.
- [7] Li, Zhen, Jinglei Yang, Zheng Liu, Xiaomin Yang, Gwanggil Jeon, and Wei Wu. "Feedback network for image super-resolution." In *Proceedings of the IEEE/CVF conference on computer vision and pattern recognition*, pp. 3867-3876. 2019.
- [8] Dai, Tao, Jianrui Cai, Yongbing Zhang, Shu-Tao Xia, and Lei Zhang. "Second-order attention network for single image super-resolution." In *Proceedings of the IEEE/CVF conference on computer vision and pattern recognition*, pp. 11065-11074. 2019.
- [9] Zhao, Xiaole, Ying Liao, Tian He, Yulun Zhang, Yadong Wu, and Tao Zhang. "FC²N: Fully Channel-Concatenated Network for Single Image Super-Resolution." *arXiv preprint arXiv:1907.03221* (2019).
- [10] Hou, Biao, Kang Zhou, and Licheng Jiao. "Adaptive super-resolution for remote sensing images based on sparse representation with global joint dictionary model." *IEEE Transactions on Geoscience and Remote Sensing* 56, no. 4 (2017): 2312-2327.
- [11] Chang, Kan, Pak Lun Kevin Ding, and Baoxin Li. "Single image super-resolution using collaborative representation and non-local self-similarity." *Signal processing* 149 (2018): 49-61.
- [12] Zhang, Yulun, Yapeng Tian, Yu Kong, Bineng Zhong, and Yun Fu. "Residual dense network for image super-resolution." In *Proceedings of the IEEE conference on computer vision and pattern recognition*, pp. 2472-2481. 2018.
- [13] Zhang, Yulun, Kungpeng Li, Kai Li, Lichen Wang, Bineng Zhong, and Yun Fu. "Image super-resolution using very deep residual channel attention networks." In *Proceedings of the European conference on computer vision (ECCV)*, pp. 286-301. 2018.
- [14] Haris, Muhammad, Gregory Shakhnarovich, and Norimichi Ukita. "Deep back-projection networks for super-resolution." In *Proceedings of the IEEE conference on computer vision and pattern recognition*, pp. 1664-1673. 2018.
- [15] Lei, Sen, Zhenwei Shi, and Zhengxia Zou. "Super-resolution for remote sensing images via local-global combined network." *IEEE Geoscience and Remote Sensing Letters* 14, no. 8 (2017): 1243-1247.
- [16] Tong, Tong, Gen Li, Xiejie Liu, and Qinquan Gao. "Image super-resolution using dense skip connections." In *Proceedings of the IEEE international conference on computer vision*, pp. 4799-4807. 2017.
- [17] Kim, Jiwon, Jung Kwon Lee, and Kyoung Mu Lee. "Accurate image super-resolution using very deep convolutional networks." In *Proceedings of the IEEE conference on computer vision and pattern recognition*, pp. 1646-1654. 2016.
- [18] Dong, Chao, Chen Change Loy, Kaiming He, and Xiaoou Tang. "Image super-resolution using deep convolutional networks." *IEEE transactions on pattern analysis and machine intelligence* 38, no. 2 (2015): 295-307.
- [19] Yang, Daiqin, Zimeng Li, Yatong Xia, and Zhenzhong Chen. "Remote sensing image super-resolution: Challenges and approaches." In *2015 IEEE international conference on digital signal processing (DSP)*, pp. 196-200. IEEE, 2015.
- [20] Zhang, Hongyan, Zeyu Yang, Liangpei Zhang, and Huanfeng Shen. "Super-resolution reconstruction for multi-angle remote sensing images considering resolution differences." *Remote Sensing* 6, no. 1 (2014): 637-657.
- [21] Yuan, Qiangqiang, Li Yan, Jiancheng Li, and Liangpei Zhang. "Remote sensing image super-resolution via regional spatially adaptive total variation model." In *2014 IEEE Geoscience and Remote Sensing Symposium*, pp. 3073-3076. IEEE, 2014.

- [22] Gou, Shuiping, Shuzhen Liu, Shuyuan Yang, and Licheng Jiao. "Remote sensing image super-resolution reconstruction based on nonlocal pairwise dictionaries and double regularization." *IEEE Journal of Selected Topics in Applied Earth Observations and Remote Sensing* 7, no. 12 (2014): 4784-4792.
- [23] Zhang, Yingying, Wei Wu, Yong Dai, Xiaomin Yang, Binyu Yan, and Wei Lu. "Remote sensing images super-resolution based on sparse dictionaries and residual dictionaries." In *2013 IEEE 11th International Conference on Dependable, Autonomic and Secure Computing*, pp. 318-323. IEEE, 2013.
- [24] Shah, Amisha J., and Suryakant B. Gupta. "Image super resolution-a survey." In *2012 1st International Conference on Emerging Technology Trends in Electronics, Communication & Networking*, pp. 1-6. IEEE, 2012.
- He, Chu, Longzhu Liu, Lianyu Xu, Ming Liu, and Mingsheng Liao. "Learning based compressed sensing for SAR image super-resolution." *IEEE Journal of Selected Topics in Applied Earth Observations and Remote Sensing* 5, no. 4 (2012): 1272-1281.

